Supplementary Information

Filamentous fungi control multiphase flow and fluid distribution in heterogeneous porous media

Sang Hyun Lee[1,2], Marcel Moura[3], Shreya Srivastava[1], Cara Santelli[1,4], Peter K. Kang[1,5*]

[1]Department of Earth and Environmental Sciences, University of Minnesota - Twin Cities, Suite 150, 116 Church St SE, Minneapolis, MN,55455, USA.
[2]Department of Microbiology, University of Massachusetts Amherst, 416 Morrill Science Center 4 North, 639 North Pleasant Street, Amherst, MA 01003 USA.
[3]PoreLab, the Njord Center, Department of Physics, University of Oslo, P.O. Box 1074 Blindern, 0316 Oslo, Norway.
[4]BioTechnology Institute, University of Minnesota - Twin Cities, 1479 Gortner Avenue Suite 140 St. Paul, MN 55108-6106
[5]Saint Anthony Falls Laboratory, University of Minnesota - Twin Cities, 2 3rd Ave SE, Minneapolis, MN, 55414 USA.

*Corresponding author(s). E-mail(s): pkkang@umn.edu;
Contributing authors: sanghyunlee@umass.edu; marcel.moura@fys.uio.no; sriva215@umn.edu; santelli@umn.edu;

Table of content:

1. Microbiome analysis of biofilm from local coal-tar contaminated site
2. Analysis of NAPL volume change via direct consumption
3. Randomization of pillars
4. Fungal colony permeability analysis
5. Analysis of hydrophobicity of Penicillium sp. MLAC-nap12
6. Supplementary Discussion: Fingering pattern of pore invasion
7. Supplementary Table
8. Supplementary Captions of Movies
9. Supplementary References

1. Microbiome analysis of biofilm from local coal-tar contaminated site

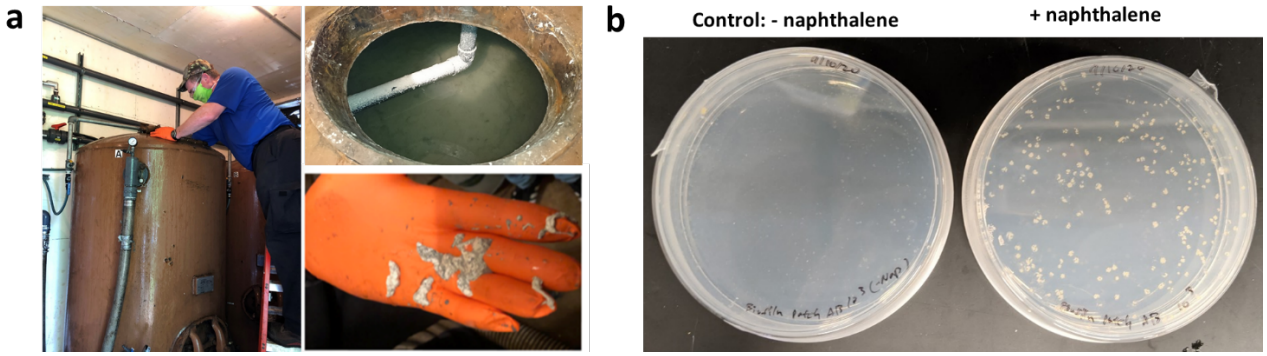

Fig. S1. a) white, slimy biofilm formed in the granulated activated carbon tank of the treatment facility, and b) the naphthalene-degrading fungal colony, Penicillium sp. MLAC-nap12*, was isolated from the biofilm using culture enrichment technique. The ITS sequencing indicated that the genus Penicillium was the predominant fungal genus in the sampled biofilm.*

The naphthalene-degrading fungi, *Penicillium* sp. MLAC-nap12, used in this study was isolated the biofilm formed in the granulated activated carbon (GAC) tanks at the on-site treatment facility of a local coal-tar contaminated site. Our microbiome analysis indicated that *Penicillium* genus was abundant in multiple locations of GAC tanks and groundwater. The microbiome analysis was conducted as follows. DNA was extracted from 500 mg of biofilm sample using FastDNA Spin kit for soil (MP Biomedicals, CA, USA) with the following modifications to the manufacturer's instructions. To minimize inhibition by metal(loid) cations, polyadenosine (200 µg) was added to the lysis buffer following the methods described in previous studes[1,2]. Two homogenization steps were conducted on the FastPrep instrument (MP Biomedicals, CA, USA), with a 5-minute incubation in ice between the steps. The centrifugation step to remove soil and cell debris was extended to 15 minutes, and the incubation period for the binding matrix was extended to 10 minutes. DNA elution was performed by resuspending the binding matrix in 80 µL of nuclease-free sterile water and incubating at 55°C for 15 minutes. Negative controls were also included to check for contaminants in the sterile water or the kits. DNA quantification was done using the Qubit double-stranded DNA broad-range (BR) assay kit (Life Technologies, USA) with a Qubit 2.0 fluorometer (Life Technologies, USA), and samples exceeding 100 ng/µL were diluted to that concentration. The DNA extracts from each triplicate sample for each depth per location duplicate were pooled into a single sample and stored at -20°C until DNA sequencing.

The amplification and sequencing of microbiome marker genes were conducted at the University of Minnesota Genomics Center using a dual-indexing technique adapted from the Earth Microbiome Project protocols on the Illumina MiSeq platform[3]. For the fungal internal transcribed spacer region (ITS1), ITS1F and ITS2R primers were used[4]. All DNA samples were purified with Ampure bead SPRI Cleanup (Beckman Coulter, CA, USA) before amplification. Post-amplification, the DNA samples underwent 2 x 300 bp paired-end sequencing using the MiSeq reagent v3 600-cycle kit (Illumina, San Diego, CA, USA).

Mothur software package (version 1.45.3)[5] was used to process the raw DNA reads according to the protocol described by Kozich et al.[6]. The fungal ITS reads were classified using the

assembled contig sequences against the UNITE+INSD database (version 8.0)[7,8] and clustered into OTUs with a 97% sequence similarity cutoff using vsearch in mothur[9]. Only OTUs with more than 10 sequences were considered for further analysis to minimize the potential inclusion of artifacts from rare OTUs[10]. The sequence count of each OTU present in the negative controls (DNA extraction and PCR amplification) was manually subtracted from the sequence abundance of that OTU for fungi using R version 3.6.3 (R Core Team).

The resulting abundance ranking, at the genus level, of the fungal community in the biofilm sampled from the site was *Penicillium, Aspergillus, Rhodotorula, Alternaria, and Cladosporium* in descending order. The *Penicillium* genus was also found in groundwater sampled from the contaminated wells. These results suggest that the fugal strain used in this study has a high survival chance when applied to a real site.

2. Analysis of NAPL volume change via direct consumption

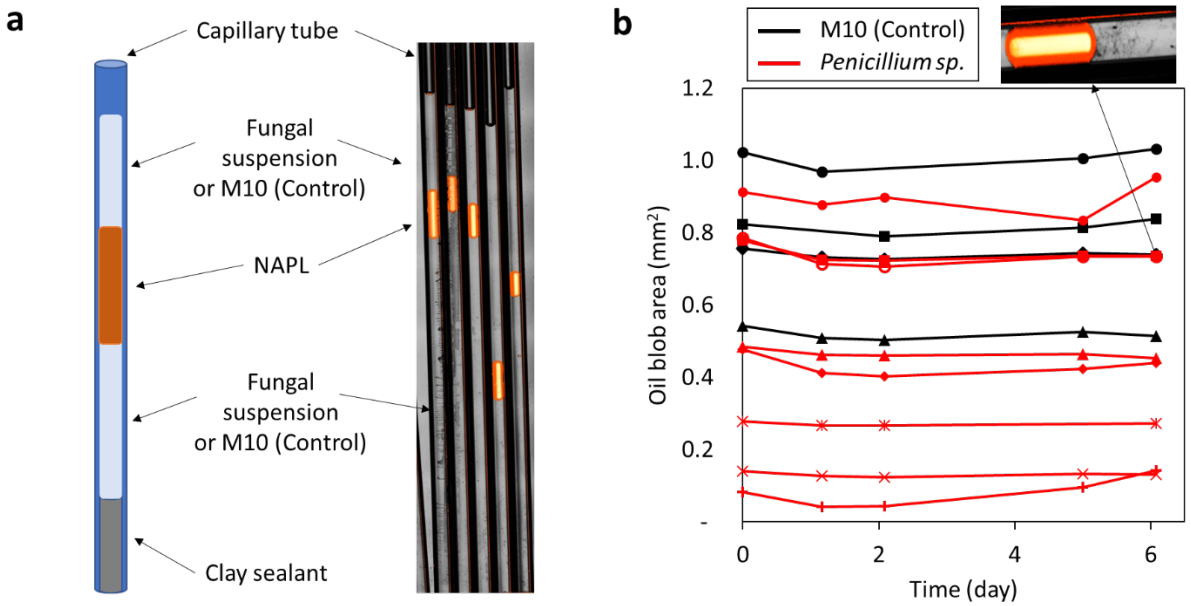

Fig. S2. NAPL volume change by the direct consumption of oil by Penicilium sp. was not significant. a) schematics showing the incubation of fungal suspension in micro-capillary tubes with NAPL for monitoring of oil blob size under microscope at room temperature and b) plot of oil blob area change over 6-day period demonstrate insignificant impact on the oil volume change by fungal consumption.

The volume change by the direct consumption of NAPL by the fungi was assessed through observing the area of NAPL blob in contact with fungal particles in micro-capillary tubes. The inner diameter of the capillary was 500 µm and the capillary was loaded with components as the sequence of aqueous solution, NAPL, aqueous solution, and clay sealant (Fig. S2a). The aqueous solution was either sterile M10 medium as the control or the blended fungal suspension in M10 while 0.1 g/L of naphthalene was dissolved in the NAPL. Blending of the fungal suspension is described in the main manuscript. Four capillaries were loaded without

fungi while eight capillaries were filled with fungal suspension. Loaded capillaries were incubated under room temperature and periodically imaged via microscope. The operation of microscope and the analysis of NAPL area was conducted as described in the Methods section of the main manuscript.

The result indicates that there is no notable reduction in the oil blob area in both control and fungi-loaded capillaries over a 6-day period (Fig. S2b). A closer look at the blobs shows direct contact between fungi and NAPL (inset). Moreover, Movies S5 and S6 indicate the displacement of oil phase upon penetration of fungal hyphae. These data collectively infer that the apparent reduction in the NAPL in the microfluidic experiment was not due to consumption of NAPL by the fungi.

3. Randomization of pillars

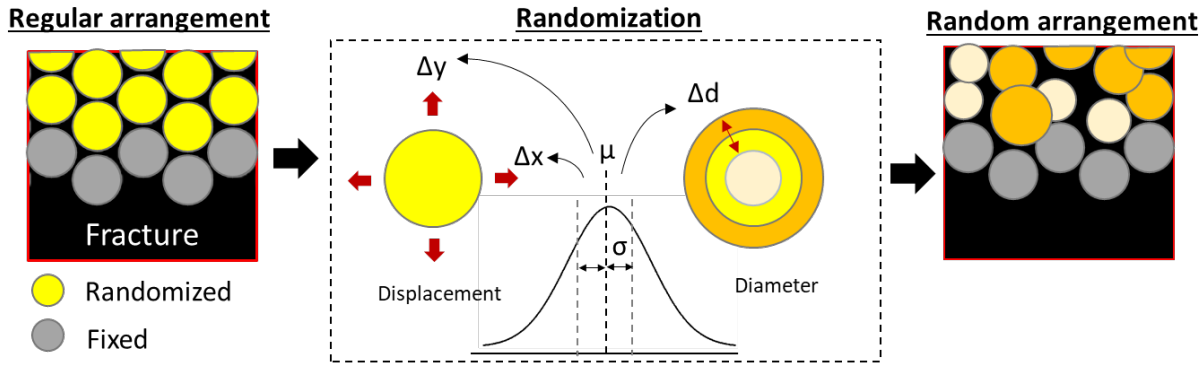

Fig. S3. Schematics of pillar randomization. For displacement, two numbers, Δx and Δy in μm, are randomly sampled from a normal distribution with a mean, μ, of 0 μm and standard deviation, σ, of 5 μm and added to x and y coordinates of pillars in the regularly arranged porous media system. Diameter is randomized by replacing the diameter value from the regular arrangement with a random value sample from a normal distribution with μ = 50 μm, and σ = 10 μm. Overlapping of cylinders was allowed as shown in the schematics in the right. The pillars interfacing the fracture are remained fixed to maintain the initial capillary entry pressure and fracture aperture identical to the regularly arranged porous media case.

4. Fungal colony permeability analysis

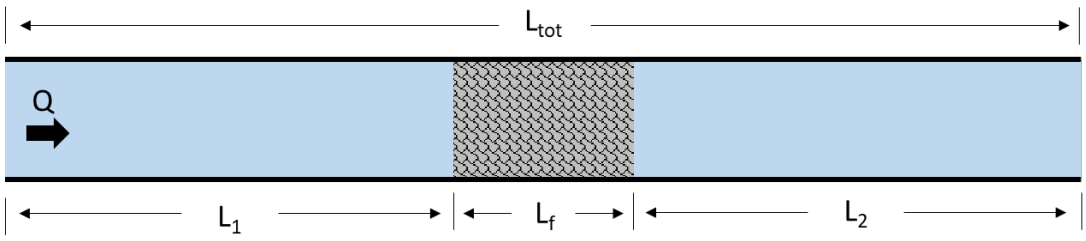

Fig. S4. Conceptual diagram of fungal clogged conduit for estimation of fungal permeability.

The permeability of a fungal colony was estimated by applying Darcy's law in a hypothetical conduit colonized by a fungal colony as shown in Fig. S4. This system corresponds to the condition before the

pore invasion in the dual-porosity chip. Hence, this approach allows analysis of fungal permeability before the invasion takes place. The pressure drop across the channel is $\Delta P_{tot} = \Delta P_{L1} + \Delta P_f + \Delta P_{L2}$ where subscripts *L1* and *L2* represent channel segments before and after the clogged region which is denoted by the subscript *f* and total channel length, L_{tot}, equals sum of L_1, L_2, and L_f. ΔP_{tot} is the measured pressure difference between the inlet and outlet. Darcy's law describes the pressure drop across the empty channel, ΔP_0, as:

$$\Delta \boldsymbol{P_0} = \frac{\boldsymbol{Q}}{\boldsymbol{A}} \frac{\boldsymbol{\mu}}{\boldsymbol{k_0}} \boldsymbol{L_{tot}}$$

where Q is the flow rate, A is the cross-sectional area of the main channel, μ is dynamic viscosity of water at 23°C (0.93 mPa· s), and k_0 is the permeability of empty channel. Our measurement of pressure drop before growth of fungi yielded k_0 of 11.9 darcy which is comparable to previously reported value of fractured rocks with apertures greater than 100 μm[11]. Upon growth of fungi, the pressure drop across the total length of the chip, ΔP_{tot}, becomes:

$$\Delta \boldsymbol{P_{tot}}(\boldsymbol{t}) = \frac{\boldsymbol{Q}}{\boldsymbol{A}} \frac{\boldsymbol{\mu}}{\boldsymbol{k_0}} \left(\boldsymbol{L_{tot}} - \boldsymbol{L_f}(\boldsymbol{t}) \right) + \frac{\boldsymbol{Q}}{\boldsymbol{A}} \frac{\boldsymbol{\mu}}{\boldsymbol{k_f}(\boldsymbol{t})} \boldsymbol{L_f}(\boldsymbol{t})$$

where L_f is the colony size and k_f is the permeability of fungal colony in darcy. Combining the two equations above yields $k_f(t)$:

$$\boldsymbol{k_f}(\boldsymbol{t}) = \frac{\boldsymbol{k_0}}{\left(\frac{\Delta \boldsymbol{P_{tot}}(\boldsymbol{t})}{\Delta \boldsymbol{P_0}} - \mathbf{1} \right) \frac{\boldsymbol{L_{tot}}}{\boldsymbol{L_f}(\boldsymbol{t})} + \mathbf{1}}$$

The colony size was analyzed by fitting the Gaussian curve to the projected intensity profile of fungal colony along the channel length and taking the three sigma and the density of the fungal colony was obtained by dividing the area under the intensity profile (total biomass amount) by the colony size (Fig. 4a). The permeability of fungal colony was calculated between 17th and 25th hour from which the fungal colony fully covered the aperture of the main flow channel (around the 17th hour) until the first pore invasion at which our assumption of straight conduit breaks, and flow starts to become diverted (Fig. 4c).

5. Analysis of hydrophobicity of *Penicillium* sp. MLAC-nap12

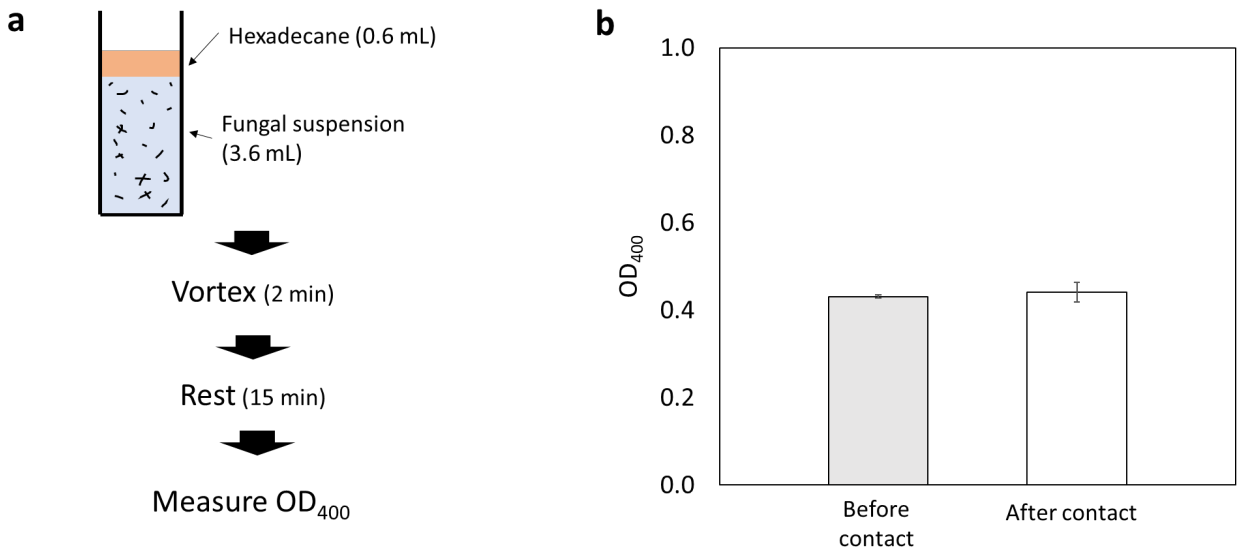

Fig. S6. Microbial Adhesion To Hydrocarbon (MATH) test showed that Penicillium sp. is hydrophilic. a) schematics of MATH test protocol and b) fungal particle concentrations estimated by optical density at 400 nm, OD_{400}, in the aqueous phase before and after contact with hexadecane indicate that fungi preferentially partition in aqueous phase. Average values are plotted and the error bars are the standard deviation (n = 4).

The Microbial Adhesion To Hydrocarbon (MATH) test[12] was performed to test the hydrophobicity of the surfaces of the fungi. The protocol is depicted in Fig. S6a. In detail, 3.6 mL of the blended fungal suspension was contacted with 0.6 mL of hexadecane in a conical tube and the mixture is vortexed for 2 minutes. The solution is set to rest for 15 minutes and the optical density at 400 nm, OD_{400}, of the aqueous phase was measured and compared to that before contact with the NAPL to assess the concentration of fungal particles in the water. The result in Fig. S6b shows that almost all fungal particles remained in the aqueous phase. This indicates that the fungal strain used in this study is hydrophilic.

In addition, Movie S7 shows an invaginated shape of an oil blob in water on a glass surface upon poking by a hyphal tip at 2.4 hour. This is attributed to the hydrophilic nature of the fungal surface which gave rise to the displacement of oils shown in the movie and throughout the study.

6. Supplementary Discussion: Fingering pattern of pore invasion

The viscosity ratio and capillary number are calculated to interpret the fingering behavior of the pore invasion in regular and random pillar arrangements. The viscosity ratio M was approximately 1:54 (water:NAPL)[13] which resulted in log M of -1.7. The capillary number, *Ca*, was estimated by $Ca = \frac{\mu_{NAPL} u_{def}}{\gamma}$, where μ_{NAPL} is the viscosity of NAPL, u_{def} is the velocity of the defending phase during invasion, and γ is the NAPL-water interfacial energy. Our estimation from analyzing the pore invasion length between 30-minute interval recorded consecutive

images yielded an average invasion velocity of 4.5×10^{-7} m/s. The resulting range of Ca was 1.1×10^{-6} which yielded log Ca of -6.0. Assessing these values with previously reported data[14] indicates that our system is in the transition regime between viscous and capillary fingering. It is noteworthy that the morphology of fingering in the regular pillar arrangement chip resembles that of viscous fingering (Fig. 1c) while that in the randomized porous media chip resembles more of capillary fingering (Fig. 3c). To the best of authors' knowledge, this is the first report of the fingering displacement pattern of wetting phase by invading phase induced by microbes.

7. Supplementary Table

Table S1. Contact angle and pendant drop analysis to test production of biosurfactant that can alter contact angle and interfacial energy. The contact angle was measured by generating a droplet of aqueous phase on a flat PDMS surface submerged in the oil phase while pendant drop analysis was conducted with an aqueous droplet at the tip of a needle submerged in the oil phase. Total five independent samples were analyzed and the average and standard deviation are tabulated.

	Contact angle (°)	Interfacial energy (mN/m)
Filtered fungal solution	150 (± 0.7)	22.7 (± 0.4)
M10 (control)	152 (± 1.0)	22.5 (± 0.3)

8. Supplementary Captions of Movies

Movie S1. Clogging of the main channel by filamentous fungi drives displacement of NAPL from model fractured aquifer system. The top panel shows the overview of the dual-porosity chip, the middle panel displays the invasion area color-coded with time-of-change, and the bottom panel shows the pressure drop and the volume of displaced oil from the chip. The experiment was performed as described in the methods section in the chip with regularly arranged pillars. The color coding by the time-of-change was performed by assigning the time value to the pixels of newly invaded area of binarized images.

Movie S2. Invasion of NAPL-filled pores with large throats by penetration of multiple hydrophilic hyphae. Images were recorded after the syringe pump was stopped once the fungal colony attached and started to grow in the chip with regularly arranged pillars. The pore throat or distance between pillars was 100 μm.

Movie S3. Filamentous fungi-enhanced oil displacement is reproduced in randomized porous media. The top panel shows the overview of the dual-porosity chip, and the bottom panel shows zoomed in video of area colonized by a fungus, and the pressure drop and the volume of displaced oil from the chip. The experiment was performed as described in the methods section in the chip with randomly arranged pillars.

Movie S4. Alteration of oil blob shape by poking of hydrophilic hyphal tip. Images were recorded after the syringe pump was stopped once the fungal colony attached and started to grow in the main flow channel. The oil blob shown with white outline sits on the glass surface in water saturated conduit. The change in the oil blob's shape upon contact with hyphae shows their hydrophilic nature.

Movie S5. Invasion of NAPL-filled pores with small throats by penetration of a single hydrophilic hypha. Images were recorded after the syringe pump was stopped once the fungal colony attached and started to grow in the chip with regularly arranged pillars. The pore throat or distance between pillars was 10 µm.

Movie S6. Hydrophilic hypha induced pore invasion at a single pore level. Images were recorded after the syringe pump was stopped once the fungal colony attached and started to grow in the chip with regularly arranged pillars. The pore throat or distance between pillars was 10 µm.

Movie S7. Split of oil island or bridging of water via hyphal penetration. Images were recorded after the syringe pump was stopped once the fungal colony attached and started to grow in the chip with regularly arranged pillars. The pore throat or distance between pillars was 10 µm.

9. Supplementary References

1. Webster, G., Newberry, C. J., Fry, J. C. & Weightman, A. J. Assessment of bacterial community structure in the deep sub-seafloor biosphere by 16S rDNA-based techniques: a cautionary tale. *J. Microbiol. Methods* **55**, 155–164 (2003).
2. Rosenfeld, J. A. *et al.* Genome assembly and geospatial phylogenomics of the bed bug Cimex lectularius. *Nat. Commun.* **7**, 10164 (2016).
3. Gohl, D. M. *et al.* Systematic improvement of amplicon marker gene methods for increased accuracy in microbiome studies. *Nat. Biotechnol.* **34**, 942–949 (2016).
4. Tedersoo, L. *et al.* Shotgun metagenomes and multiple primer pair-barcode combinations of amplicons reveal biases in metabarcoding analyses of fungi. *MycoKeys* **10**, 1–43 (13AD).
5. Schloss, P. D. *et al.* Introducing mothur: open-source, platform-independent, community-supported software for describing and comparing microbial communities. *Appl. Environ. Microbiol.* **75**, 7537–7541 (2009).
6. Kozich, J. J., Westcott, S. L., Baxter, N. T., Highlander, S. K. & Schloss, P. D. Development of a dual-index sequencing strategy and curation pipeline for analyzing amplicon sequence data on the MiSeq Illumina sequencing platform. *Appl. Environ. Microbiol.* **79**, 5112–5120 (2013).
7. Nilsson, R. H. *et al.* The UNITE database for molecular identification of fungi: handling

dark taxa and parallel taxonomic classifications. *Nucleic Acids Res.* **47**, D259–D264 (2019).

8. Kõljalg, U. *et al.* Towards a unified paradigm for sequence-based identification of fungi. *Mol. Ecol.* **22**, 5271–5277 (2013).
9. Rognes, T., Flouri, T., Nichols, B., Quince, C. & Mahé, F. VSEARCH: a versatile open source tool for metagenomics. *PeerJ* **4**, e2584 (2016).
10. Brown, S. P. *et al.* Scraping the bottom of the barrel: are rare high throughput sequences artifacts? *Fungal Ecol.* **13**, 221–225 (2015).
11. Lamur, A. *et al.* The permeability of fractured rocks in pressurised volcanic and geothermal systems. *Sci. Rep.* **7**, 6173 (2017).
12. Rosenberg, M., Barki, M., Bar-Ness, R., Goldberg, S. & Doyle, R. J. Microbial adhesion to hydrocarbons (math). *Biofouling* **4**, 121–128 (1991).
13. Noureddini, H., Teoh, B. C. & Davis Clements, L. Viscosities of vegetable oils and fatty acids. *J. Am. Oil Chem. Soc.* **69**, 1189–1191 (1992).
14. Zhang, C., Oostrom, M., Wietsma, T. W., Grate, J. W. & Warner, M. G. Influence of Viscous and Capillary Forces on Immiscible Fluid Displacement: Pore-Scale Experimental Study in a Water-Wet Micromodel Demonstrating Viscous and Capillary Fingering. *Energy and Fuels* **25**, 3493–3505 (2011).